ORGANOMETALLICS

ARTICLE

pubs.acs.org/Organometallics

Cyclopentadienylphosphazene (CpPN) Complexes of Rare-Earth Metals: Synthesis, Structural Characterization, and Hydroamination Catalysis

Noa K. Hangaly,[‡] Alex R. Petrov,[‡] Konstantin A. Rufanov,[‡,§] Klaus Harms,[‡] Michael Elfferding,[‡] and Jörg Sundermeyer*[,‡]

[‡]Fachbereich Chemie der Philipps-Universität Marburg, Hans-Meerwein-Strasse, 35032 Marburg, Germany

[§]Department of Chemistry, M.V. Lomonosov State University of Moscow, 119992, Moscow, Russia

Supporting Information

ABSTRACT:

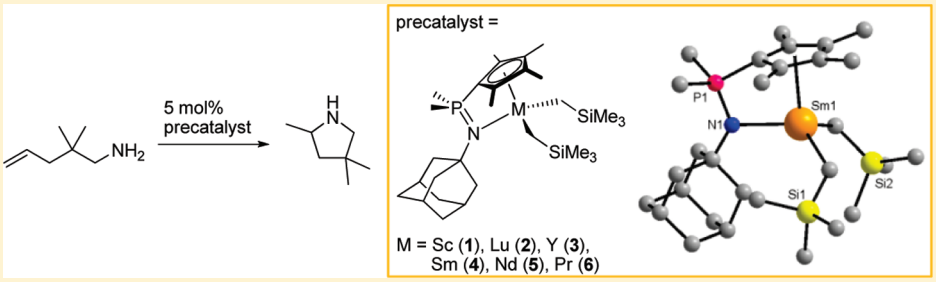

Synthesis of the first series of rare-earth-metal constrained geometry complexes containing the *P*-(1-adamantylamino)-*P*-dimethyl-tetramethyl-cyclopentadienylidene-phosphorane ligand $C_5Me_4PMe_2NHAd$, $\{Cp^{\#}PN\}H$, was accomplished. This monoanionic chelate ligand is isoelectronically related to the classical dianionic cyclopentadienyl-silylamine ligand $C_5Me_4HSiMe_2NHtBu$, $\{Cp^{\#}SiN\}H_2$. The ligand stabilizes dialkyls $[\{Cp^{\#}PN\}M(CH_2SiMe_3)_2]$ (M = Sc, **1**; Lu, **2**; Y, **3**; Sm, **4**; Nd, **5**; Pr, **6**; Ce, **7**) over the full range of group 3 and lanthanide cation radii. Results of NMR studies of these crystalline alkyls, XRD molecular structures, and a preliminary study revealing the high catalytic activity of complexes **3**−**6** in the intramolecular hydroamination/cyclization are reported. The catalytic experiments reveal a trend in activity Lu < Y < Sm < Nd ≤ Pr resembling the trend in rare-earth-metal radii. Interestingly they reveal a distinctive substrate-dependent first-order kinetic profile for all metals investigated. The reaction of the precatalyst **3** with 1.6 equiv of the standard substrate 2,2-dimethylpenten-4-ylamine leads to a fast and selective formation of substrate complex $[\{Cp^{\#}PN\}Y(NHCH_2CMe_2CH_2CH{=}CH_2)_2]$ (**8**). Fast cyclization was observed only after addition of more than 2 equiv of amine substrate. A noninsertive mechanism involving a six-membered transition state by a concerted C−N bond formation and N−H bond cleavage at a 3:1 substrate to complex ratio is suggested on the basis of these findings.

INTRODUCTION

For a long time, organometallic chemistry and catalysis of rare-earth metals[1] has largely been dominated by metallocenes.[2] More recently, considerable attention has been directed toward rare-earth-metal *mono*-cyclopentadienyl complexes providing an electronically more unsaturated and a sterically less crowded reactive site, thus showing unique reactivities that differ significantly from those of the metallocenes.[3] The research led, *inter alia*, to an extensive study of a wide range of Cp substitution patterns. One of the great achievements in half-sandwich complex design is the constrained geometry complexes (CGCs), which contain a short side arm bearing an additional chelating donor functionality at the Cp ligand.[4] CGCs with the cyclopentadienyl-silylamido (CpSiN)-type ligands, initially developed by Bercaw[5] and Okuda,[6] became one of best developed classes of these half-sandwich complexes. In particular, their titanium complexes are highly active single-site olefin polymerization and copolymerization catalysts.[7] By changing the bridging atom in CpSiN from Si to P^+, monoanionic cyclopentadienyl-phosphazene ligands (CpPN) are generated, which are isoelectronically related to classical dianionic CpSiN ligands. Previously, we reported a convenient and general synthetic protocol for the synthesis of a large variety of CpPN-type ligands with different substitution pattern at N and P atoms and at the Cp ring, their spectroscopic properties and molecular structures, and investigations on the tautomeric equilibria of their protonated forms.[8] Their use in the stabilization of highly reactive alkyls of rare-earth and group 4 metals has been claimed,[9] and a representative CpPN lutetium alkyl complex has been presented.[10] Independently, related fluorenyl- and indenyl-phosphazene ligands (FluPN and IndPN) and their rhodium[11] and zirconium[12]

Received: March 25, 2011
Published: August 11, 2011

Scheme 1. Isolobal Relationship between CpSiN- and CpPN-Type Complex Families

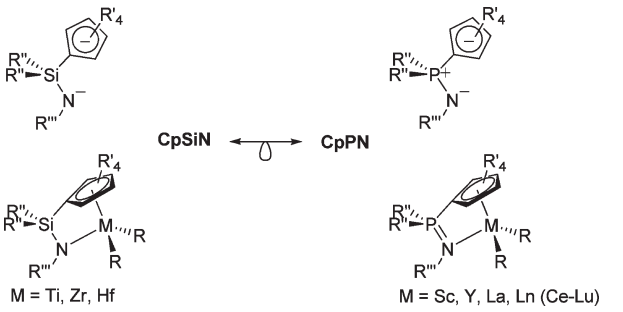

Scheme 2. CGCs of Rare-Earth Metals

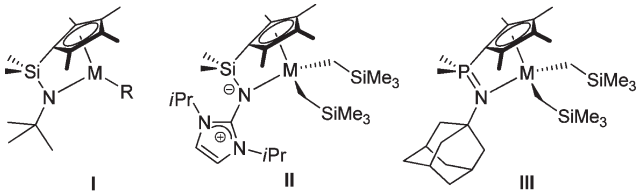

complexes were presented by Bourissou and co-workers. Theoretical investigations of CpPN-type complexes of group 4 elements suggest them to be interesting alternatives for CpSiN-derived catalysts.[13]

CpSiN complexes of tetravalent group 4 elements are isoelectronic to CpPN complexes of trivalent group 3 elements and isolobal to trivalent lanthanide complexes (Scheme 1).

Having this concept in mind and considering the advantage of rare-earth metals offering a unique and gradual variation of their properties relating to their decreasing radii, we initiated a research program aimed at evaluating organometallic chemistry of rare-earth-metal CpPN complexes.[10,14]

The simple catalytic addition of a N−H bond to an unsaturated C−C bond, the hydroamination reaction, represents a prominent, highly atom-efficient, and elegant reaction for the synthesis of higher substituted nitrogen-containing products. Particularly, intramolecular hydroamination/cyclizations represent an efficient route for accessing multifunctional nitrogen-containing heterocycles for construction of a range of biologically active molecules and naturally occurring alkaloids.[15] Since the seminal discovery of organolanthanide metallocene-catalyzed hydroamination by Marks and co-workers,[16] rare-earth metals have proven to be very active for intra-[16,17] and intermolecular[17f,18] hydroamination of alkenes. Catalytic activity is enhanced by both increasing the Ln^{3+} radii of the precatalysts and improved coordination sphere accessibility.[16c,17j,17k] Lanthanide CpSiN constrained geometry complexes of type I (Scheme 2) have been shown to exhibit markedly increased activity in catalytic intramolecular hydroamination/cyclization processes by creating a more open coordination sphere with better access to the metal center relative to lanthanocenes and *ansa*-lanthanocenes.[19,15e] Moreover, rare-earth-metal complexes with Me_2Si-bridged cyclopentadienyl-imidazolin-2-imine ligands (type II) studied by Tamm and co-workers showed catalytic activities in the intramolecular hydroamination/cyclization.[20]

Scheme 3. Synthesis of $Cp^{\#}PN$ Complexes 1−7

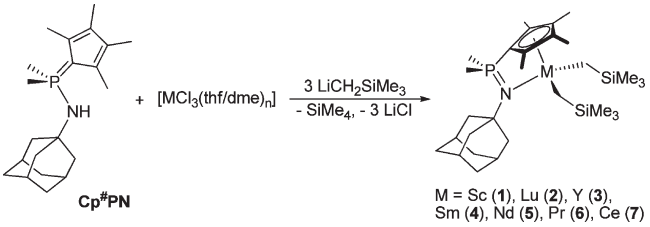

These complexes also exhibit a zwitterionic ligand structure like the CpPN complexes of type III. For this reason we were interested in investigating the catalytic performance of the $Cp^{\#}PN$ complexes of type III.

Here we describe the synthesis, NMR spectroscopic studies, and molecular structures of the first series of CpPN-type constrained geometry complexes with *P*-(1-adamantylamino)-*P*-dimethyl-tetramethyl-cyclopentadienylidene-phosphorane, $C_5Me_4{=}PMe_2NHAd$ ($\{Cp^{\#}PN\}H$), using a representative pool of rare-earth metals (Sc, Lu, Y, Sm, Nd, Pr, and Ce). In addition, preliminary results of their application in olefin hydroamination catalysis are presented. It was shown that these reactive organolanthanide complexes efficiently mediate intramolecular hydroamination/cyclization reactions under mild conditions.

RESULTS AND DISCUSSION

Synthesis of Rare-Earth-Metal Dialkyl CpPN Complexes. In our first report we applied a protocol for direct metalation of $\{Cp^{\#}PN\}H$ with $[Lu(CH_2SiMe_3)_3(thf)_2]$ that allowed us to obtain the desired CpPN complex $[\{Cp^{\#}PN\}Lu(CH_2SiMe_3)_2]$ in nearly quantitative yield.[10] However, only a few rare-earth-metal tris-alkyl precursors are of sufficient thermal stability.[21] Therefore, we have used an alternative synthetic protocol that comprises addition of 3 equiv of $LiCH_2SiMe_3$ to a stirred suspension of an equimolar mixture of $\{Cp^{\#}PN\}H$ ligand and rare-earth-metal halide source $[ScCl_3(thf)_3]$ or $[MCl_3(dme)_n]$ (M = Lu, Y, Sm ($n = 2$); M = Nd, Pr, Ce ($n = 1$)) in ether/hexane or ether/toluene mixtures at 0 °C (Scheme 3). One equivalent of the lithium alkyl is acting as a base, and the other two are acting as nucleophiles. Applying this method and this sterically demanding ligand, only complexes with a ligand:metal = 1:1 ratio were isolated, whereas in other cases metallocenes with a 2:1 ratio were obtained.[14]

An appropriate workup (filtration, solvent removal, extraction with hexane followed by crystallization) gave air-sensitive $[\{Cp^{\#}PN\}M(CH_2SiMe_3)_2]$, M = Sc (**1**), Lu (**2**), Y (**3**), Sm (**4**), Nd (**5**), Pr (**6**), and Ce (**7**) complexes. These rare-earth-metal dialkyls were isolated as microcrystalline solids of analytical purity in 50−90% yields. The complexes **1**−**7** show moderate solubility in saturated hydrocarbons and are highly soluble in etheric and aromatic solvents. Not surprisingly, the thermostability of the complexes depends on the metal center ionic radius. Colorless alkyl complexes of metals with smaller radii, **1**−**3** (Sc, Lu, Y), possess high thermostability. They can be stored under inert atmosphere at ambient temperature for months without noticeable decomposition. Fast decomposition takes place at temperatures above 150 °C. Complexes containing larger metal ions **4**−**6** (Sm, Nd, and Pr) are thermally stable at −30 °C for months, but in solution they decompose gradually at 25 °C and completely within 6 h at 50 °C. The cerium complex

dx.doi.org/10.1021/om200264n |*Organometallics* 2011, 30, 4544–4554

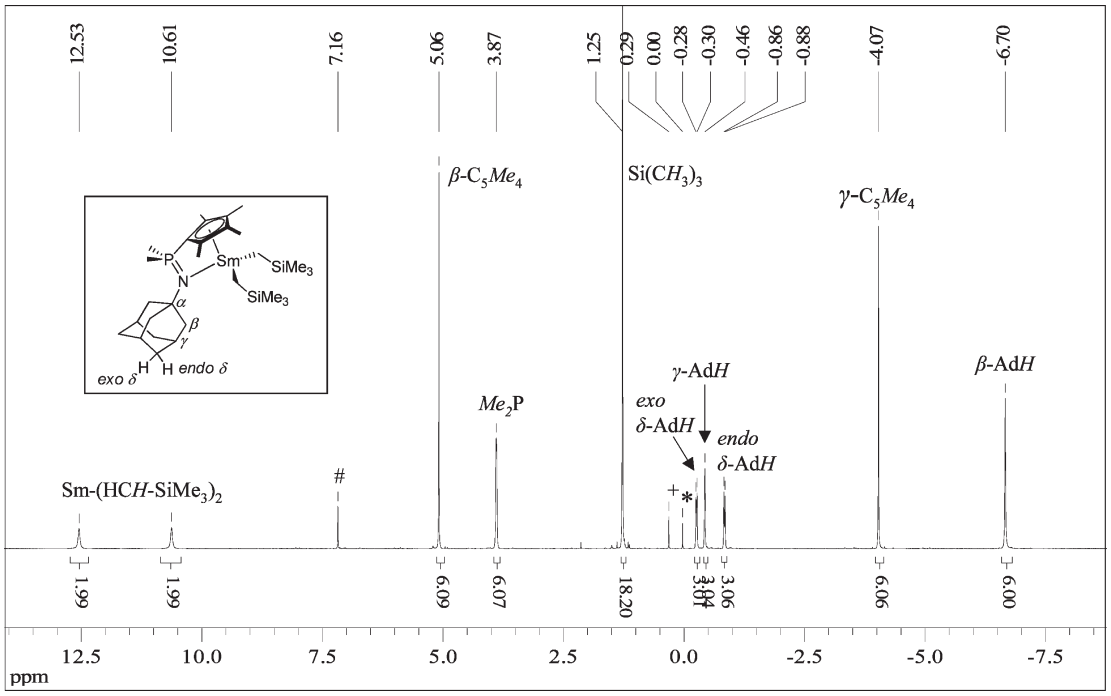

Figure 1. ^{1}H NMR spectrum (500.1 MHz) of samarium complex **4** in C_6D_6 at 27 °C. Signals denoted with (*), (+), and (#) are assigned to TMS, silicon grease, and the residual protons of C_6D_6.

7 shows the lowest thermal stability and decomposes readily at ambient temperature, which did not allow obtaining the correct elemental analysis.

Multinuclear NMR Spectroscopy of Cp$^{\#}$PN Complexes 1−7. All complexes were characterized by multinuclear NMR spectroscopy. According to the ^{1}H and ^{13}C{^{1}H} NMR spectroscopy, **1**−**7** were isolated without coordinated ether molecules, which are present in the starting material. Compared with the free ligand {Cp$^{\#}$PN}H (δ_P = 17.6 ppm),[10] the ^{31}P{^{1}H} NMR signals of diamagnetic **1**−**3** are only slightly shifted upfield and appear in the region between δ_P = 9.0 and 9.6 ppm. The ^{31}P{^{1}H} NMR resonances of the paramagnetic complexes **4**−**7** are broad, nevertheless clearly assigned as signals at δ_P = 25.3 (**4**), −3.9 (**7**), −59.0 (**6**), and −89.3 (**5**), respectively.

^{1}H NMR spectra of the diamagnetic complexes **1**−**3** are very similar, and therefore only the spectrum of representative yttrium complex **3** is further discussed. Its ^{1}H NMR spectrum at room temperature is rather simple (see Supporting Information), showing two resonances at δ_H = 2.03 and 2.11 ppm assigned to the equivalent pairs of methyl protons of the C_5Me_4 moiety, a typical set of adamantyl signals at δ_H = 1.56, 1.71, and 2.00 ppm with an integral ratio of 6:6:3, and the doublet of the Me_2P protons at δ_H = 1.16 ppm ($^{2}J_{HP}$ = 12.5 Hz). The silylmethylene protons are magnetically nonequivalent and appear as two doublets of doublets at δ_H = −0.70 and −0.75 ppm ($^{2}J_{HH}$ = 11.1 Hz, $^{2}J_{HY}$ = 3.0 Hz) at +25 °C. Analogously in the ^{1}H NMR spectra of complex **1** and complex **2** two signals for diastereotopic methylene protons of CH_2SiMe_3 groups at δ_H = −0.38, −0.34 and δ_H = −0.95, −0.89 ppm, respectively, were observed.

The assignment of the NMR signals for the paramagnetic complexes **4**−**7** requires analysis of two-dimensional NMR spectra due to the paramagnetic shift. The signals observed in the ^{1}H NMR spectra recorded in C_6D_6 at 25 °C are spread over a wide range up to Δppm of 139 (δ_H = 92 to −47 ppm) for f^2Pr^{3+} complex **6** (δ_H = 13 to −7 ppm for f^5Sm^{3+} (**4**), δ_H = 30 to −22 ppm for f^3Nd^{3+} (**5**), and 44 to −23 ppm for f^1Ce^{3+} (**7**)). In general, the relative arrangement of the signals in these spectra is very similar, and therefore the spectrum of complex **4** is discussed as a representative example (Figure 1).[22]

Generally, the resonances in the spectrum of **4** are narrow except the two broad resonances for the diastereotopic methylene protons of the Me_3SiCH_2 group, which are significantly downfield shifted to values of 10.61 and 12.53 ppm. All resonances of the adamantyl protons are shifted upfield. The diastereotopic geminal *exo*- and *endo*-δ-methylene protons of the Ad group appear at δ_H = −0.29 and −0.87 ppm, respectively, as two doublets ($^{2}J_{HH}$ = 11.6 Hz). The signal of the γ-methine protons also appears in that region (−0.46 ppm), presumably due to the comparable distance to the paramagnetic metal center. The β-methylene protons of the adamantyl group situated close to the samarium atom reveal significantly upfield shifted resonances (−6.70 ppm). One set of chemically equivalent methyl protons of the C_5Me_4 moiety appears as downfield- and the other as upfield-shifted resonances (5.06 and −4.07 ppm). Such signal distribution was previously observed in the closely related homoleptic complex [Sm{C_5Me_4H}$_3$] (0.82 and −5.70 ppm).[23] ^{1}H NMR spectra of corresponding neodymium, praseodymium, and cerium complexes also show up- and downfield-shifted resonances for the C_5Me_4 moiety at δ_H = 11.44 and −13.52 ppm for **5** (cf. [Nd{C_5Me_4H}$_3$]:[24] δ_H = 16.64 and −16.68 ppm), δ_H = 25.94 and −30.25 ppm for **6**, and δ_H = 11.89 and −14.77 ppm for **7**, respectively.

To date, ^{13}C NMR resonance assignment and a detailed analysis for paramagnetic lanthanide organometallics are discussed rarely in the literature. The analysis was performed on complexes **4** and **5**. The assignment of resonances of the high-resolution ^{13}C{^{1}H} NMR spectra was accomplished by 2D HMBC and HSQC experiments.[22] Unambiguous assignment

of C_5Me_4 methyl groups was achieved by HMBC spectroscopy (Figure 2), resulting in the resonance at 5.06 ppm being assigned to β-C_5Me_4 and those at −4.07 ppm to γ-C_5Me_4 methyl protons.

Molecular Structures of Cp#PN Complexes. Single crystals of **1**, **3**, and **4** were obtained by cooling saturated hexane solutions to −30 °C. Their molecular structures are closely related to that of the earlier reported lutetium complex **2**.[10] They crystallize in the monoclinic space groups $P2_1/c$ (**1**) and $P2_1/n$ (**3**, **4**) with four molecules in the unit cell (Figure 3). Selected bond lengths (Å) and angles (deg) for **1**−**4** are presented in Table 1. In the case of complex **1** the CH_2SiMe_3 groups are disordered and treated with an occupancy factor of 87:13.

In the solid state **1**, **3**, and **4** adopt mononuclear structures, in which metal atoms are approximately in tetrahedral coordination. The P−C_{C1} bond lengths (1.753−1.774 Å) are longer than in the free ligand (1.724(2) Å),[10] while the P−N bonds are essentially shorter (1.594−1.623 Å) than in the free aminophosphonium ylide ligand (1.659(2) Å).[10]

The M−N bond distances (Sc−N 2.185(2) Å; Y−N 2.316(4) Å; Sm−N 2.366(3) Å) are short and approach the distance typically found for amido complexes. They are only slightly longer than the covalent M−N bonds in CGCs of the type [{CpSiN}M(R)(L)] (M = Sc: 2.083 Å;[5b] Y: 2.208(6) Å;[25] Sm: 2.343(4) Å)[26] and of homoleptic amido complexes [M{N($SiMe_3$)$_2$}$_3$] (for M = Sc: av 2.05 Å;[27] Y: av 2.22 Å;[28] Sm: av 2.28 Å).[29] Typically, simple donor−acceptor complexes such as [{Me_3TACN}M(CH_2SiMe_3)$_3$] reveal much longer average M−N bonds: Sc−N 2.47 Å and Y−N 2.60 Å.[30] The relatively strong donor capacity of the chelating phosphazene nitrogen atom, expressed by the short M−N distance, corresponds with only little stabilization of the anionic charge at nitrogen by the phosphonium center. This is also shown by a rather long P−N distance of 160.0 ± 1.0 Å.

The M−Cp_{centr} and the average M−CH_2 bond lengths are comparable to those reported for other complexes containing η^5-C_5Me_4[26] and CH_2SiMe_3 ligands (cf. complexes of Sc;[31] Y;[32] Sm[33]).

Furthermore, the Cp_{centr}−M−N angles (97.6° for **1**; 91.5° for **3**; 89.4° for **4**) are clearly smaller than the Cp_{centr}−M−N angles in closely related CpSiN alkyl complexes (M = Sc: 104.4°; Y: 96.4°; Sm: 94.3°).[26]

Catalytic Hydroamination/Cyclization Reactions. In order to better compare the catalytic activity of complexes **2**−**6** with those reported in literature, we studied the transformation of standard ω-aminoalkene substrates 2,2-dimethyl- and 2,2-diphenylpenten-4-ylamine (**S1** and **S2**, respectively) under similar conditions to those reported for reference compounds of CGC of type I and II (Scheme 2). The reactions were carried out in C_6D_6 at 27 or 60 °C with ca. 5 mol % catalyst loading and were monitored by *in situ* ^{1}H NMR spectroscopy. The results are summarized in Table 2.

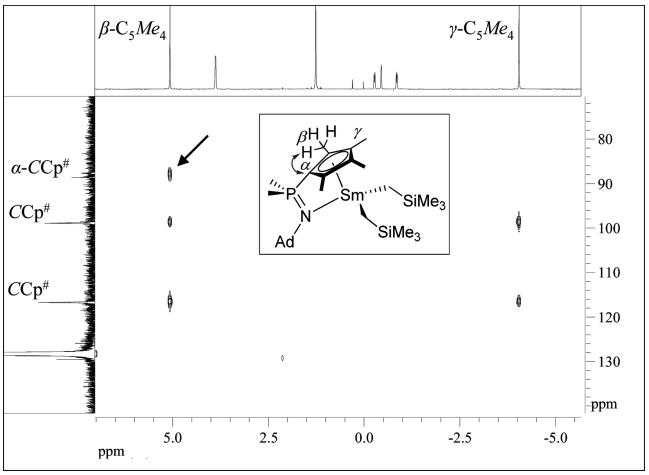

Figure 2. Section of the HMBC spectrum of complex **4** in C_6D_6 at 27 °C. The ^{1}H NMR spectrum (500.1 MHz) is shown at the top and the ^{13}C{^{1}H} NMR spectrum (125.8 MHz) is shown on the left edge in the contour plot.

Table 1. Selected Bond Lengths and Angles for Complexes 1−4

	1 (Sc)	**2** (Lu)[10]	**3** (Y)	**4** (Sm)
		Bond Lengths (Å)		
M−N	2.185(2)	2.278(3)	2.316(4)	2.367(3)
M−C1	2.431(2)	2.545(4)	2.599(3)	2.642(3)
M−Cp_{centr}	2.235	2.285	2.392	2.450
M−C12	2.243(3)	2.360(4)	2.416(5)	2.472(3)
M−C16	2.234(3)	2.358(4)	2.434(5)	2.469(4)
P−N	1.606(2)	1.600(3)	1.605(4)	1.593(3)
P−C1	1.769(3)	1.774(4)	1.753(6)	1.774(3)
		Bond Angles (deg)		
C1−M−N	68.0(1)	65.2(1)	63.3(1)	62.4(1)
Cp_{centr}−M−N	97.6	95.8	91.5	89.4
C12−M−N	108.4(1)	109.9(2)	106.6(2)	119.9(1)
C16−M−N	114.6(1)	115.9(2)	118.5(1)	107.5(1)
C12−M−C16	107.5(1)	109.9(2)	111.5(2)	113.1(1)

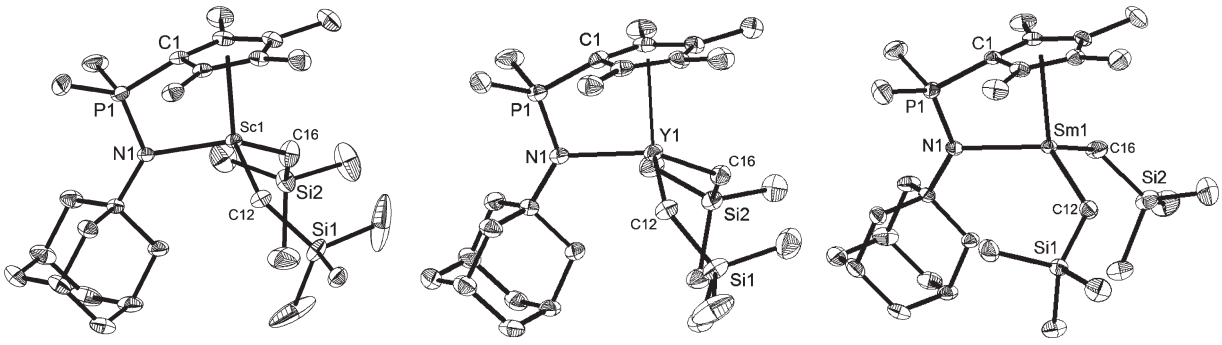

Figure 3. ORTEP diagram of scandium (**1**), yttrium (**3**), and samarium (**4**) Cp#PN complexes with 30% thermal ellipsoids. All hydrogen atoms have been omitted for clarity. In structure **1**, disordered Me_3SiCH_2 groups with lower occupancies have also been omitted.

dx.doi.org/10.1021/om200264n |*Organometallics* 2011, 30, 4544–4554

Table 2. Catalytic Intramolecular Hydroamination/Cyclization by Complexes 2 (Lu), 3 (Y), 4 (Sm), 5 (Nd), and 6 (Pr)

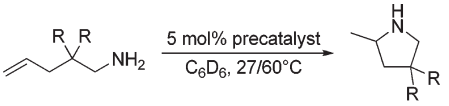

R = Me (**S1**), Ph (**S2**)

entry	precatalyst (mol %)	substrate	T (°C)	t (h)	conversion (%)[a]
1	**2** (5.8)	**S1**	27	15.75	36
2	**2** (6.0)	**S1**	60	14.19	>92
3	**3** (5.0)	**S1**	27	4.58	>93
4	**3** (5.2)	**S2**	27	0.25	>92
5	**3** (5.0)	**S1**	60	1.37	>92
6	**4** (5.0)	**S1**	27	0.98	>93
7	**5** (5.3)	**S1**	27	0.47	>93
8	**6** (5.3)	**S1**	27	0.40	>93

[a] Conversion to pyrrolidine (yield) assigned by ^{1}H NMR spectroscopy with respect to ferrocene. Note that in entries 2−8 substrates were quantitatively converted by the precatalyst, but under these conditions ca. 10 mol % substrate is consumed to form the active catalyst species (*vide infra*).

Complexes **3**−**6** are active catalysts and show almost full conversion at 27 °C. Increasing the Ln^{3+} ionic radius leads to significant reaction rate enhancement (Figure 4, A). Complexes of smaller ionic radii rare-earth metals **1** (Sc) and **2** (Lu) have a low catalytic activity in hydroamination/cyclization reactions of substrate **S1** at room temperature. Complex **2** achieves a conversion of only 36% after about 16 h, but at elevated temperature the reaction rate dramatically increases and shows conversion of 92% after about 14 h at 60 °C (Table 2, entries 1 and 2; Figure 4, B). Yttrium complex **3** shows a conversion of 93% for substrate **S1** after 4.6 h and an almost quantitative hydroamination after only 0.25 h for substrate **S2** (Table 2, entries 3 and 4), where the Thorpe−Ingold effect[34] is more pronounced. Elevated reaction temperatures also increase the reaction rate, and complex **3** shows almost quantitative conversion after 1.4 h for **S1** at 60 °C (Table 2, entry 5; Figure 4, B). The complexes with larger metal cations **4**−**6** display much higher activities. They show a near-quantitative conversion after only 60, 28, and 24 min (Table 2, entries 6−8; Figure 4, A), respectively, following the trend, the lager the ionic radii, the higher the rate of conversion, as often observed in rare-earth-metal-catalyzed hydroamination/cyclization reactions.[16c,17j,17k]

This preliminary study reveals that CGCs of the larger rare-earth metals (samarium, neodymium, and praseodymium) can be used as efficient hydroamination/cyclization precatalysts. A direct comparison of CpPN-type III CGCs with other CGC types is difficult due to their different kinetic profile in olefin hydroamination. The conversion values with the CpPN precatalysts are dependent on substrate concentration and not independent such as with catalysts of the CpSiN-type with zero-order kinetic profiles. Their initial activity compares well to the activities found for CGC alkyls and amides of type I[19] and II[20] (Scheme 2). Due to the first-order kinetics, the productivity decreases significantly at higher conversions; as a consequence, long reaction times are necessary for completion of the reaction. Additional testing on nonactivated substrates and variation of catalyst loading (<5 mol %) are required.

Mechanistic Consideration of First-Order Mechanism. The most intriguing feature of the CpPN catalysts of type III is a

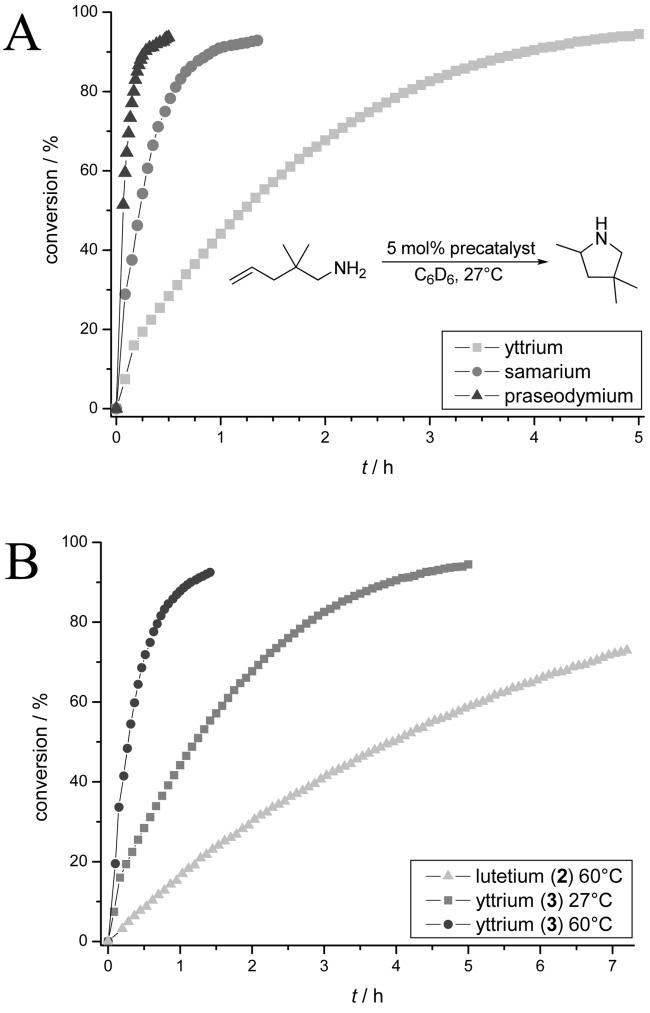

Figure 4. (A) Conversion to pyrrolidine (yield) as a function of time for hydroamination/cyclization of **S1** using complexes of yttrium (**3**, squares), samarium (**4**, circles), and praseodymium (**6**, triangles). The plot of neodymium complex **5** is too close to the one of **6** and not shown for clarity. (B) Conversion versus time plots for the hydroamination/cyclization of **S1** at 60 °C using precatalyst **2** (triangles) and precatalyst **3** at 27 °C (squares) and 60 °C (circles).

dramatic and constant deviation from zero-order rate law, which is typically observed for lanthanocenes and CGCs of type I and is commonly explained by the olefin insertion into the M−N bond being the rate-determining step.[17c−m,19] In contrast, all precatalysts **3**−**6** show a distinctive first-order dependence on substrate concentration over almost the entire conversion range, more precisely up to at least 85% conversion. A representative first-order kinetic plot ($-\ln([S]/C_{0,S})$ vs t) for complex **3** is shown in Figure 5. The other precatalysts follow the same kinetic reaction pattern and are given in the Supporting Information. In all cases the data could be convincingly fit ($R^2 > 0.998$) by the least-squares method.

The "pure" first-order kinetics over the full range of conversion has rarely been observed in rare-earth-metal complex catalysis. Deviations from zero-order kinetics are often observed at higher substrate conversions (>50%) when sterically more accessible *ansa*-lanthanocenes[17] and CGC−Ln systems[17h,i,19] were employed. This deviation has been attributed to the coordination of the Lewis basic product, leading to competitive product

dx.doi.org/10.1021/om200264n |*Organometallics* 2011, 30, 4544–4554

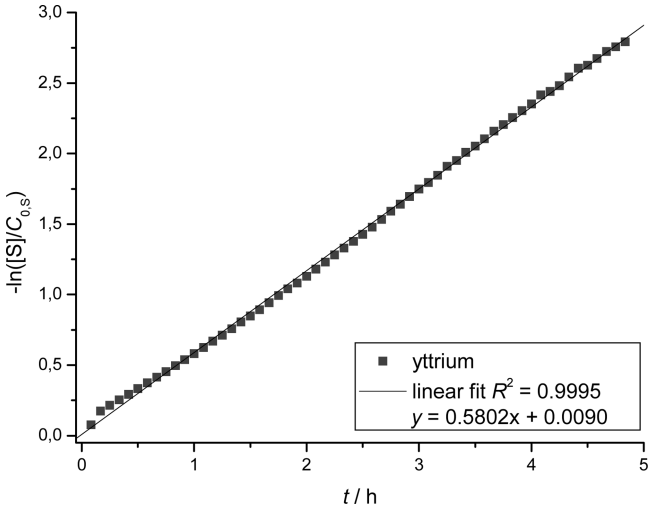

Figure 5. Kinetic plot $-\ln([S]/C_{0,S})$ as a function of time for **S1** using precatalyst **3** in C_6D_6 (27 °C). The line represents the least-squares fit to the data points.

inhibition. First-order kinetics have been observed by Hessen and his group using nitrogen ligand based cationic and neutral non-metallocene rare-earth-metal complexes as precatalysts.[35,36] Interestingly, hydroamination/cyclization study of CGC of type II also shows a significant deviation from ideal zero-order kinetics.[20]

Hultzsch and co-workers reported a first-order rate dependence on substrate concentration for biphenolate and binaphtholate rare-earth-metal amide complexes.[37] However, a later study clearly showed zero-order kinetics for analogous alkyl complexes. As a consequence, the first-order dependence was related to a hampered catalyst activation step due to the amide ligand present in the precatalyst.[38] We can exclude this explanation in our case: According to *in situ* ^{1}H NMR spectroscopy, the initial reaction step is a rapid and quantitative aminolysis of both alkyl groups by the primary amine substrates. This was shown by an immediate formation of 2 equiv of free $SiMe_4$. In order to observe this reaction in more detail, we studied the stoichiometric model reaction. The reaction of the yttrium precatalyst **3** with only 1.6 equiv of the amine substrate **S1** leads at room temperature to a fast and selective formation of $[\{Cp^{\#}PN\}Y(NHCH_2CMe_2CH_2CH{=}CH_2)_2]$ (**8**) characterized by NMR spectroscopy. The $^{31}P\{^1H\}$ NMR spectrum shows a new signal at δ_P = 6.7 ppm; the double bonds in the ^{1}H NMR spectrum are represented by signals at δ_H = 5.10−5.19 and 6.01−6.12 ppm. No cyclization at room temperature was observed; however addition of a third equivalent of amine substrate (or any excess > 2 equiv) to **8** leads to the formation of free pyrrolidine product next to the active catalyst **8**. No secondary amido complex of the product or alkyl complex of an insertive pathway was observed.

Previously, $[Cp'_2La(NHR)(NH_2R)]$ (R = $CH_2CMe_2CH_2$-$CH{=}CH_2$) was characterized at low temperatures (−60 °C) by means of NMR spectroscopy. At ca. −20 °C cyclization occurs and $[Cp'_2La(NR'')(HNR'')]$ (R″ = $-CH_2C(CH_3)_2CH_2-C(CH_3)H-$) was isolated and characterized.[16c]

Our privileged spectator ligand system allows us to monitor the catalyst conversion via $^{31}P\{^1H\}$ and ^{1}H NMR spectroscopy. *In situ* $^{31}P\{^1H\}$ NMR spectroscopic studies of reactions with all five precatalysts under conditions given in Table 2 indicate that the CpPN ligand is strongly bonded to the metal center, since no

Scheme 4. Synthesis of $Cp^{\#}$PN Diamidoalkene Complex 8

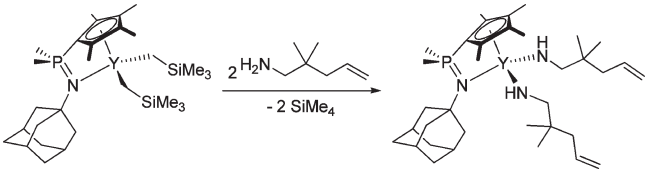

formation of protonated ligand (δ_P = 17.6 ppm)[10] was observed by $^{31}P\{^1H\}$ NMR spectroscopy over the full reaction time. Moreover, *in situ* $^{31}P\{^1H\}$ and ^{1}H NMR spectroscopic studies indicate that complex **8** is also present during the reaction among the other species. Furthermore, at a catalyst load of 5 mol %, we observed that the productivity decreases significantly at high conversions of about 90%. This might be because about 10 mol % of the amine is consumed to form the diamido catalyst species without any product formation. *In situ* ^{1}H NMR experiments reveal that both the substrate and the product are in rapid equilibrium with the catalytically active species, as both substrate and product amines resonances are paramagnetically broadened during turnover for Sm^{3+} ($4f^5$) and in particular for Nd^{3+} ($4f^3$) and Pr^{3+} ($4f^2$) catalysts. A fast substrate and product exchange on the NMR time scale at room temperature is in accord with the literature on other HA catalysts.[16c,17i,17m]

There are a few possible mechanistic variations discussed for organolanthanide-mediated hydroamination/cyclization. The common mechanism involves a rate-determining intramolecular insertion of the olefin into the metal−nitrogen bond.[17c−m,19] An alternative mechanistic variation is a noninsertive mechanism that involves coordination of an additional substrate molecule for cyclization. A noninsertive mechanism was originally suggested by Marks and co-workers to account for the observed strong primary kinetic isotope effects (KIE) in Cp_2Ln-catalyzed hydroamination of aminoalkenes.[16c] For organoactinide-catalyzed hydroamination Marks and co-workers again suggested that protonolysis may be concurrent with cyclization.[39] Recently, Sadow and co-workers suggested a concerted C−N and C−H bond formation in a magnesium-catalyzed hydroamination reaction. They supported it with kinetic studies and isolated magnesium amidoalkenes, which did not react without a slight excess of substrate.[40] Moreover, Hill and his group suggested a mechanism involving a concerted proton transfer step associated with rate-determining alkene insertion in alkaline earth-metal-catalyzed ω-aminoalkene hydroamination.[41] Sadow[42] and Scott[43] discussed such a mechanism for ω-aminoalkene hydroamination by zirconium compounds. Furthermore, comprehensive computational insights on the most closely related system—organolanthanide-mediated hydroamination of conjugated ω-aminodienes and allenes—were provided by Tobisch, recently.[44]

Based on the experimental kinetic observations and the stoichiometric model reaction, we favor a noninsertive mechanism for CpPN rare-earth-metal dialkyl- or diamido-mediated hydroamination catalysis (Scheme 5). Coordination of a third amine substrate at high amine concentration is competitive or even inhibitive with respect to olefin coordination to a hard d^0 metal center. In an insertive mechanism, coordination of a third amine substrate to the catalyst $[\{Cp^{\#}PN\}M(NHR)_2]$ **B** generating $[\{Cp^{\#}PN\}M(NHR)_2(NH_2R)]$ **C** would probably suppress metal−olefin interaction, whereas in a noninsertive mechanism, coordination of the third amine would be required for ring-closure. Moreover, the low activity of catalysts with smallest ionic

dx.doi.org/10.1021/om200264n |*Organometallics* 2011, 30, 4544–4554

Scheme 5. Suggested Noninsertive Mechanism for Intramolecular Hydroamination/Cyclization of ω-Aminoalkenes by CpPN Rare-Earth-Metal Complexes[45]

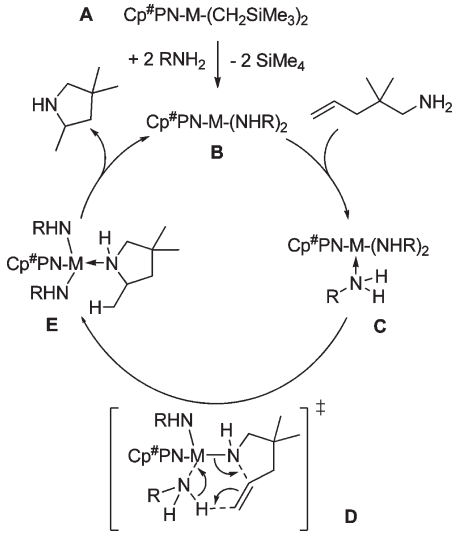

radii could be explained by the fact that larger cations should be able to bind more easily an additional primary amine, forming species **C**. The latter could act as the strongest NH acid in the system and could promote a concerted proton transfer to the olefinic double bond via a six-membered transition state **D** involving a three-electron-pair shift. The result of this transformation would be a conversion of a primary amine complex **C** into a secondary amine complex **E**, which further dissociates into the product and the catalytically active bis-amido species **B**.

The key transformation step **C** → **E** is strongly dependent on the concentration of the substrate compared to the concentration of the product, and it could explain the observed first-order kinetics as supported by the model cyclization reaction with active species **8**. This proposal does not exclude that a critical dissociation step of the secondary amine complex **E** with regeneration of the catalyst **B** could lead to product inhibition, but it offers an alternative to the common view that proton transfer is directed toward a carbanion that was formed via olefin insertion into the M−N bond.

CONCLUSIONS

This study reveals that monoanionic cyclopentadienylphosphazene Cp#PN is a privileged ligand to effectively stabilize dialkyl constrained geometry complexes of small, medium, and large rare-earth-metal ions. A straightforward one-pot synthesis of complexes of the type [{η^5,η^1-$C_5Me_4PMe_2NAd$}M-$(CH_2SiMe_3)_2$], M = Sc (**1**), Lu (**2**), Y (**3**), Sm (**4**), Nd (**5**), Pr (**6**), and Ce (**7**), was achieved without the necessity for isolation of homoleptic Ln alkyls or a lithiated Cp#PN ligand. For this purpose etherates of the rare-earth-metal halides and protonated ligand are treated with 3 equiv of $LiCH_2SiMe_3$; thereby two of them act as nucleophiles and one as a base. All complexes were thoroughly characterized by NMR spectroscopy, including the signal assignment of the paramagnetic complexes **4**−**7**. Furthermore, **1**−**4** were structurally characterized and support the strongly chelating constrained geometry character of these cyclopentadienyl-phosphazene ligands. Only η^1,η^5-coordination of the ligand was observed with small as well as with larger rare-earth-metal cations. No coordination of additional donors such as thf even for Cp#PN alkyls of the larger cations is observed. The Cp#PN ligand has a strong M−N bonding and a considerably smaller Cp_{centr}−M−N angle compared to CpSiN complexes. Hydroamination/cyclization reactions on two representative ω-penten-4-ylamines, 2,2-dimethyl- (**S1**) and 2,2-diphenylpenten-4-ylamine (**S2**), were investigated. The activity measured under identical conditions increases with increasing ionic radii in the order $Lu^{3+} < Y^{3+} < Sm^{3+} < Nd^{3+} \leq Pr^{3+}$. Complexes of smaller ionic radii rare-earth metals **1** (Sc) and **2** (Lu) have a low catalytic activity in hydroamination/cyclization reactions at room temperature. Complexes with larger ionic radii, **4**−**6**, were found to be catalysts of high activity. The catalytic activity increases dramatically at higher reaction temperatures. In contrast to other literature known CGCs we do not observe a zero-order rate dependence on substrate concentration and characteristic deviations at higher conversions, but we observe a distinctive substrate-dependent first-order kinetic profile up to high conversions. Furthermore, the active catalyst species [{Cp#PN}$Y(NHCH_2CMe_2CH_2CH{=}CH_2)_2$] (**8**) formed upon rapid aminolysis of yttrium precatalyst **3** with less than 2 equiv of aminoalkene **S1** was characterized by NMR. No cyclization at ambient temperature was observed for **8**. However, addition of a third equivalent of amine substrate to **8** leads to the formation of free pyrrolidine product, while the observed concentration of the active catalyst in the reaction mixture remains constant.

Our observations of a distinctive substrate-dependent first-order kinetic profile, the strong correlation of activity to the ionic radii and higher coordination number associated with larger cations, and the stoichiometric model reaction let us suggest a concerted noninsertive mechanism with a proton transfer from a coordinated acidic primary amine to the olefin. Three electron pairs shifted via a six-membered transition state convert a primary amine substrate complex to a ring-closed secondary amine product complex. This proposal requires further support by measuring kinetic isotope effects and by computational studies. Furthermore, these results clearly indicate the necessity and opportunity to tune this new class of CGCs for catalytic hydroamination of Thorpe−Ingold nonactivated substrates by variation of substituents at N, P, and the Cp ring as well as by the size of the metal cation.

EXPERIMENTAL SECTION

General Procedures. All manipulations were performed under purified argon or nitrogen using standard high-vacuum or Schlenk techniques, or in a glovebox. Solvents were dried and distilled under argon employing standard drying agents. All organic reagents were purified by conventional methods. NMR spectra were recorded at 300 K on a Bruker ARX200, Bruker DPX250, Bruker AMX300, Bruker AVANCE DRX400, and Bruker DRX500. Elemental analyses were performed at the Analytical Laboratory of the Chemistry Department/Philipps-Universität Marburg. The starting materials $[MCl_3(thf)_3]$ (M = Sc),[5c] $[MCl_3(dme)_n]$ (M = Lu, Y, Sm (n = 2); Nd, Pr, Ce (n = 1)),[46] $LiCH_2SiMe_3$,[47] $C_5Me_4PMe_2NHAd$,[10] and aminoalkenes[48] were synthesized according to the literature methods.

X-ray Crystallographic Studies. Suitable crystals in all cases were obtained by cooling a concentrated hexane solution to −30 °C. Crystal data were collected with a Stoe-IPDSI area-detector diffractometer using graphite-monochromatized Mo Kα radiation (λ = 0.71073 Å) at 150 K (**3**) and 193 K (**1**, **4**). Data reduction was carried out by using the IPDS software X-Area (Stoe).[49] The data were empirically corrected for absorption and other effects by using multiscans,[50] except for compound **3**, where no improvement in the refinement was achieved

dx.doi.org/10.1021/om200264n |*Organometallics* 2011, 30, 4544–4554

Table 3. Crystallographic Data and Structure Refinement Details for 1−4

	1	2[10]	3	4
formula	$C_{29}H_{55}NPScSi_2$	$C_{29}H_{55}LuNPSi_2$	$C_{29}H_{55}NPSi_2Y$	$C_{29}H_{55}NPSi_2Sm$
fw	549.85	679.86	593.8	655.24
temp (K)	193(2)	180(2)	150(2)	193(2)
cryst color	colorless	colorless	colorless	yellow
size (mm)	0.45 × 0.21 × 0.12	0.32 × 0.20 × 0.16	0.48 × 0.40 × 0.32	0.30 × 0.27 × 0.21
cryst syst	monoclinic	monoclinic	monoclinic	monoclinic
space group	$P2_1/c$	$P2_1/c$	$P2_1/n$	$P2_1/n$
a (Å)	15.180(1)	15.284(2)	13.360(3)	13.378(1)
b (Å)	10.344(1)	10.456(1)	17.293(3)	17.264(1)
c (Å)	20.980(2)	21.092(2)	14.497(3)	14.520(1)
α (deg)	90	90	90	90
β (deg)	92.52(1)	91.97(2)	91.26(2)	90.91(1)
γ (deg)	90	90	90	90
V (Å^3)	3291.0(4)	3368.7(7)	3348.5(19)	3353.0(5)
Z	4	4	4	4
ρ_{calcd} (g cm^{-3})	1.110	1.340	1.178	1.298
μ (mm^{-1})	0.362	3.066	1.878	1.887
no. of rflns collected	25 584	30 805	30 437	26 814
no. of indep rflns (R_{int})	6113 (0.0667)	6383 (0.0549)	5486 (0.1274)	6503 (0.0522)
GOF	0.913	1.038	0.872	0.879
R_1 ($F^2 > 2\sigma(F^2)$)	0.0462	0.0398	0.0500	0.0261
wR_2 (F^2)	0.1185	0.1034	0.1205	0.0558

through its application. The structures were solved by direct methods (Sir-92[51] and Sir-97[52]) and refined by full-matrix least-squares techniques against F_o^2 (SHELXL-97).[53] Hydrogen atoms were included in idealized positions and refined with isotropic displacement. The programs PLATON[54] and PLUTON[55] were used to check the results of the X-ray analyses. Diamond was used for structure representations.[56] CCDC-684697 (**1**), -684698 (**3**), and -791944 (**4**) contain the supplementary crystallographic data for this paper. These data can be obtained free of charge from The Cambridge Crystallographic Data Centre via www.ccdc.cam.ac.uk/data_request/cif.

General Synthetic Protocol toward [(η^5,η^1-$C_5Me_4PMe_2NAd$)M(CH_2SiMe_3)$_2$] (1−7). To a suspension of [$MCl_3(solv)_n$] (1.00 equiv) and {Cp$^{\#}$PN}H ligand (1.00 equiv) in ether was added dropwise at 0 °C a solution of $LiCH_2SiMe_3$ (ca. 3.00 equiv) in hexane (for **1**−**3**) or toluene (for **4**−**7**). The reaction mixture was stirred at 0 °C for another 0.5 h and concentrated *in vacuo* to half of the original volume. Formed LiCl was filtered off over Celite. The solvent was stripped off, and the residue was extracted with hexane. Crystallization occured by storage at −30 °C. Filtration and drying in a vacuum resulted in isolation of microcrystalline solids.

Synthesis of Scandium Complex 1. Starting from [$ScCl_3(thf)_3$] (368 mg, 1.00 mmol) and {Cp$^{\#}$PN}H (331 mg, 1.00 mmol) in 15 mL of ether and $LiCH_2SiMe_3$ (286 mg, 3.04 mmol) in 10 mL of hexane. Yield: 74% (412 mg) of a colorless solid. ^{1}H NMR (400.1 MHz, C_6D_6): δ −0.38 (d, $^2J_{HH}$ = 11.3 Hz, 2H, Sc-HC*H*), −0.34 (d, $^2J_{HH}$ = 11.3 Hz, 2H, Sc-*H*CH), 0.38 (s, 18H, Si*Me*$_3$), 1.16 (d, $^2J_{HP}$ = 12.5 Hz, 6H, *Me*$_2$P), 1.55−1.63 (m, 6H, δ-Ad*H*), 1.82−1.83 (m, 6H, β-Ad*H*), 2.01 (s, 6H, β-C_5Me_4), 2.02 (br s, 3H, γ-Ad*H*), 2.16 (s, 6H, γ-C_5Me_4) ppm. ^{13}C{^{1}H} NMR (62.9 MHz, C_6D_6): δ 4.5 (s, Si*Me*$_3$), 12.0 (d, $^4J_{CP}$ = 1.3 Hz, γ-C_5Me_4), 14.4 (s, β-C_5Me_4), 21.6 (d, $^1J_{CP}$ = 54.7 Hz, *Me*$_2$P), 30.4 (d, $^4J_{CP}$ = 1.1 Hz, γ-Ad*C*), 36.4 (s, δ-Ad*C*), 36.8 (s, Sc-CH_2), 47.2 (d, $^3J_{CP}$ = 8.6 Hz, β-Ad*C*), 54.6 (d, $^2J_{CP}$ = 6.5 Hz, α-Ad*C*), 84.8 (d, $^1J_{CP}$ = 114.0 Hz, α-C_5Me_4), 122.6 (d, $^2J_{CP}$ = 12.8 Hz, β-C_5Me_4), 125.7 (d, $^3J_{CP}$ = 14.2 Hz, γ-C_5Me_4) ppm. ^{31}P{^{1}H} NMR (121.5 MHz, C_6D_6): δ 9.5 (s) ppm. Anal. Calcd for $C_{29}H_{55}NPScSi_2$ (549.87): C 63.35, H 10.08, N 2.55. Found: 62.92, H 9.78, N 2.41.

Alternative Synthesis of Lutetium Complex 2. Starting from [$LuCl_3(dme)_2$] (232 mg, 0.50 mmol) and {Cp$^{\#}$PN}H (165 mg, 0.50 mmol) in 10 mL of ether and $LiCH_2SiMe_3$ (141 mg, 1.50 mmol) in 13 mL of hexane. Yield: 66% (225 mg) of a colorless solid. Anal. Calcd for $C_{29}H_{55}LuNPSi_2$ (679.87): C 51.23, H 8.15, N 2.06. Found: C 50.72, H 8.17, N 2.18. Spectroscopic features are in good agreement with those previously reported.[10]

Synthesis of Yttrium Complex 3. Starting from [$YCl_3(dme)_2$] (188 mg, 0.50 mmol) and {Cp$^{\#}$PN}H (165 mg, 0.50 mmol) in 10 mL of ether and $LiCH_2SiMe_3$ (143 mg, 1.52 mmol) in 10 mL of hexane. Yield: 83% (246 mg) of a colorless solid. ^{1}H NMR (300.1 MHz, C_6D_6): δ −0.75 (dd, $^2J_{HH}$ = 11.1 Hz, $^2J_{HY}$ = 3.0 Hz, 2H, Y-HC*H*), −0.70 (dd, $^2J_{HH}$ = 11.1 Hz, $^2J_{HY}$ = 3.0 Hz, 2H, Y-*H*CH), 0.38 (s, 18H, Si*Me*$_3$), 1.16 (d, $^2J_{HP}$ = 12.5 Hz, 6H, *Me*$_2$P), 1.56 (br s, 6H, δ-Ad*H*), 1.71 (s, 6H, β-Ad*H*), 2.00 (br s, 3H, γ-Ad*H*), 2.03 (s, 6H, β-C_5Me_4), 2.11 (s, 6H, γ-C_5Me_4). ^{13}C{^{1}H} NMR (75.0 MHz, C_6D_6): δ 4.7 (s, Si*Me*$_3$), 11.4 (s, γ-C_5Me_4), 13.8 (s, β-C_5Me_4), 21.9 (d, $^1J_{CP}$ = 54.9 Hz, *Me*$_2$P), 30.2 (s, γ-Ad*C*), 31.4 (d, $^1J_{CY}$ = 41.0 Hz, Y-CH_2), 36.3 (s, δ-Ad*C*), 47.6 (d, $^3J_{CP}$ = 8.7 Hz, β-Ad*C*), 54.3 (d, $^2J_{CP}$ = 6.9 Hz, α-Ad*C*), 84.6 (d, $^1J_{CP}$ = 116.1 Hz, α-C_5Me_4), 121.9 (d, $^2J_{CP}$ = 13.4 Hz, β-C_5Me_4), 123.7 (d, $^3J_{CP}$ = 14.4 Hz, γ-C_5Me_4) ppm. ^{31}P{^{1}H} NMR (121.5 MHz, C_6D_6): δ 9.0 (s) ppm. Anal. Calcd for $C_{29}H_{55}NPSi_2Y$ (593.80): C 58.66, H 9.34, N 2.36. Found: C 59.21, H 9.71, N 2.41.

Synthesis of Samarium Complex 4. Starting from [$SmCl_3$-$(dme)_2$] (437 mg, 1.00 mmol) and {Cp$^{\#}$PN}H (332 mg, 1.00 mmol) in 15 mL of ether and $LiCH_2SiMe_3$ (282 mg, 3.00 mmol) in 15 mL of toluene. Yield: 67% (402 mg) of an orange solid. ^{1}H NMR (500.1 MHz, C_6D_6): δ −6.70 (s, 6H, β-Ad*H*), −4.07 (s, 6H, γ-C_5Me_4), −0.87 (d, $^2J_{HH}$ = 11.6 Hz, 3H, *endo*-δ-Ad*H*), −0.46 (s, 3H, γ-Ad*H*), −0.29 (d, $^2J_{HH}$ = 11.6 Hz, 3H, *exo*-δ-Ad*H*), 1.25 (s, 18H, Si*Me*$_3$), 3.87 (s, 6H, *Me*$_2$P), 5.06 (s, 6H, β-C_5Me_4), 10.61 (br s, 2H, Sm-HC*H*), 12.53 (br s, 2H, Sm-*H*CH) ppm. ^{13}C{^{1}H} NMR (125.8 MHz, C_6D_6): δ 4.0 (s, Si*Me*$_3$), 4.4 (s, γ-C_5Me_4), 19.2 (s, β-C_5Me_4), 26.3 (d, $^1J_{CP}$ = 52.2 Hz, *Me*$_2$P), 26.5 (s, γ-Ad*C*), 33.5 (s, δ-Ad*C*), 39.1 (s, β-Ad*C*), 49.8 (s, α-Ad*C*), 87.3 (d, $^1J_{CP}$ = 124.3 Hz,

α-C_5Me_4), 98.6 (s, γ-C_5Me_4), 116.4 (s, β-C_5Me_4) ppm. $^{31}P\{^1H\}$ NMR (121.5 MHz, C_6D_6): δ 25.3 (br s) ppm. Anal. Calcd for $C_{29}H_{55}NPSi_2Sm$ (655.26): C 53.16, H 8.46, N 2.14. Found: C 52.28, H 8.40, N 2.38.

Synthesis of Neodymium Complex 5. Starting from [$NdCl_3$(dme)] (340 mg, 1.00 mmol) and {$Cp^{\#}PN$}H (340 mg, 1.03 mmol) in 15 mL of ether and $LiCH_2SiMe_3$ (292 mg, 3.10 mmol) in 15 mL of toluene. Yield: 49% (315 mg) of a sky blue solid. ^1H NMR (300.1 MHz, C_6D_6): δ −21.72 (s, 6H, β-Ad*H*), −13.52 (s, 6H, γ-C_5Me_4), −5.83 (d, $^2J_{HH}$ = 11.9 Hz, 3H, *endo*-δ-Ad*H*), −4.94 (s, 3H, γ-Ad*H*), −3.62 (d, $^2J_{HH}$ = 11.9 Hz, 3H, *exo*-δ-Ad*H*), 2.62 (s, 18H, $SiMe_3$), 10.58 (d, $^2J_{HP}$ = 6.0 Hz, 6H, Me_2P), 11.44 (s, 6H, β-C_5Me_4), 20.30 (br s, 2H, Nd-HC*H*), 29.62 (br s, 2H, Nd-*H*CH) ppm. $^{13}C\{^1H\}$ NMR (125.8 MHz, C_6D_6): δ −37.5 (br s, γ-C_5Me_4), −15.3 (s, β-C_5Me_4), −13.4 (s, α-AdC), 19.6 (s, γ-AdC), 27.4 (s, δ-AdC), 29.3 (s, β-AdC), 30.4 (s, $SiMe_3$), 34.7 (d, $^1J_{CP}$ = 52.7 Hz, Me_2P), 102.8 (s, γ-C_5Me_4), 107.1 (d, $^1J_{CP}$ = 124.2 Hz, α-C_5Me_4), 146.0 (s, β-C_5Me_4) ppm. $^{31}P\{^1H\}$ NMR (121.5 MHz, C_6D_6): δ −89.3 (br s) ppm. Anal. Calcd for $C_{29}H_{55}NNdPSi_2$ (649.15): C 53.65, H 8.54, N 2.16. Found: C 53.11, H 8.21, N 2.31.

Synthesis of Praseodymium Complex 6. Starting from [$PrCl_3$(dme)] (169 mg, 0.50 mmol) and {$Cp^{\#}PN$}H (166 mg, 0.50 mmol) in 10 mL of ether and $LiCH_2SiMe_3$ (142 mg, 1.51 mmol) in 15 mL of toluene. Yield: 55% (176 mg) of a pale green solid. ^1H NMR (300.1 MHz, C_6D_6): δ −46.66 (s, 6H, β-Ad*H*), −30.25 (s, 6H, γ-C_5Me_4), −13.14 (d, $^2J_{HH}$ = 10.2 Hz, 3H, *endo*-δ-Ad*H*), −12.68 (s, 3H, γ-Ad*H*), −9.33 (d, $^2J_{HH}$ = 10.9 Hz, 3H, *exo*-δ-Ad*H*), 2.96 (s, 18H, $SiMe_3$), 13.92 (d, $^2J_{HP}$ = 11.9 Hz, 6H, Me_2P), 25.94 (s, 6H, β-C_5Me_4), 86.58 (br s, 2H, Pr-HC*H*), 91.74 (br s, 2H, Pr-*H*CH) ppm. $^{31}P\{^1H\}$ NMR (121.5 MHz, C_6D_6): δ −59.0 (br s) ppm. Anal. Calcd for $C_{29}H_{55}NPPrSi_2$ (645.81): C 53.93, H 8.58, N 2.17. Found: C 53.64, H 8.83, N 2.26.

Synthesis of Cerium Complex 7. Starting from [$CeCl_3$(dme)] (168 mg, 0.50 mmol) and {$Cp^{\#}PN$}H (166 mg, 0.50 mmol) in 10 mL of ether and $LiCH_2SiMe_3$ (141 mg, 1.50 mmol) in 15 mL of toluene. Yield: 53% (171 mg) of a yellow solid. ^1H NMR (300.1 MHz, C_6D_6): δ −22.10 (s, 6H, β-Ad*H*), −14.77 (s, 6H, γ-C_5Me_4), −5.56 (d, $^2J_{HH}$ = 10.9 Hz, 3H, *endo*-δ-Ad*H*), −5.07 (s, 3H, γ-Ad*H*), −3.71 (d, $^2J_{HH}$ = 10.8 Hz, 3H, *exo*-δ-Ad*H*), 1.69 (s, 18H, $SiMe_3$), 8.43 (s, 6H, Me_2P), 11.89 (s, 6H, β-C_5Me_4), 36.86 (br s, 2H, Ce-HC*H*), 43.30 (br s, 2H, Ce-*H*CH) ppm. $^{31}P\{^1H\}$ NMR (121.5 MHz, C_6D_6): δ −3.9 (br s) ppm. The compound was found to be too unstable to record a $^{13}C\{^1H\}$ NMR spectrum and to obtain the correct values by elemental analysis.

Typical NMR-Scale Catalytic Reaction. In a N_2-filled glovebox, a NMR tube equipped with a Teflon (Young) valve was charged with 5 mol % precatalyst (0.030 mmol) and 8.0 mg of ferrocene (43.0 μmol) as internal standard dissolved in 0.6 mL of C_6D_6. On the vacuum line, the tube was evacuated while the benzene solution was frozen at ca. −60 °C. The substrate (0.60 mmol) was injected onto the solid mixture under Ar flush, and the sample maintained at −78 °C until the measurements began. The whole sample was melted and mixed just before it was placed in the Bruker Avance DRX400 spectrometer (300 or 333 K). The conversion was monitored by ^1H NMR spectroscopy by following the decrease of the olefinic signals relative to the internal standard ferrocene. NMR spectra were taken in 5, 3, or 1 min time intervals using four scans per time interval, with a 5 s delay to ensure accurate integration.

Synthesis of Yttrium Diamidoalkene Complex 8, NMR-Scale Reaction. In a N_2-filled glovebox, 17.835 mg of precatalyst **3** (30.0 μmol, 1.00 equiv) was dissolved in 0.15 mL of C_6D_6, and 5.24 mg of **S1** (46.3 μmol, 1.54 equiv) dissolved in 0.15 mL of C_6D_6 was added slowly. The mixture was transferred into an NMR tube and the reaction flasks were washed with 2 × 0.15 mL of C_6D_6. ^1H NMR (400.1 MHz, C_6D_6): δ 0.00 (s, 24H, $SiMe_4$), 1.04 (s, 12H, $NHCH_2CMe_2CH_2CH{=}CH_2$), 1.30 (d, $^2J_{HP}$ = 12.3 Hz, 6H, Me_2P), 1.61 (br s, 6H, δ-Ad*H*), 1.74 (s, 6H, β-Ad*H*), 2.02 (br s, 3H, γ-Ad*H*), 2.16 (s, 6H, γ-C_5Me_4), 2.19 (d, superposed with β-C_5Me_4, 4H, $NHCH_2CMe_2CH_2CH{=}CH_2$), 2.20 (s, 6H, β-C_5Me_4), 3.18 (d, $^3J_{HH}$ = 9.4 Hz, 4H, $NHCH_2CMe_2CH_2CH{=}CH_2$), 5.10−5.19 (m, 4H, $NHCH_2CMe_2CH_2CH{=}CH_2$), 6.01−6.12 (m, 2H, $NHCH_2CMe_2CH_2CH{=}CH_2$). $^{13}C\{^1H\}$ NMR (100.6 MHz, C_6D_6): δ 0.0 (s, $SiMe_4$), 11.2 (s, γ-C_5Me_4), 13.4 (s, β-C_5Me_4), 22.4 (d, $^1J_{CP}$ = 54.2 Hz, Me_2P), 25.3 (s, $NHCH_2CMe_2CH_2CH{=}CH_2$), 25.2 (s, $NHCH_2CMe_2CH_2CH{=}CH_2$), 30.6 (s, γ-AdC), 36.6 (s, δ-AdC), 36.7 (s, $NHCH_2CMe_2CH_2CH{=}CH_2$), 47.6 (d, $^3J_{CP}$ = 9.0 Hz, β-AdC), 52.8 (d, $^2J_{CP}$ = 7.3 Hz, α-AdC), 45.0 (s, $NHCH_2CMe_2CH_2CH{=}CH_2$), 60.9 (s, $NHCH_2CMe_2CH_2CH{=}CH_2$), 86.9 (d, $^1J_{CP}$ = 118.7 Hz, α-C_5Me_4), 115.9 (s, $NHCH_2CMe_2CH_2CH{=}CH_2$), 120.3 (d, $^2J_{CP}$ = 13.5 Hz, β-C_5Me_4), 122.7 (d, $^3J_{CP}$ = 9.1 Hz, γ-C_5Me_4), 137.6 (s, $NHCH_2CMe_2CH_2CH{=}CH_2$) ppm. $^{31}P\{^1H\}$ NMR (161.9 MHz, C_6D_6): δ 6.7 (s) ppm.

■ ASSOCIATED CONTENT

Supporting Information. Detailed NMR spectroscopic data (^1H, $^{13}C\{^1H\}$, and 2D NMR experiments) with signal assignment for complexes **3**−**6** and **8**. Figures giving representative kinetic plots. This material is available free of charge via the Internet at http://pubs.acs.org.

■ AUTHOR INFORMATION

Corresponding Author

*Phone: +49 (0)6421 2825693. Fax: +49 (0)6421 2825711. E-mail: jsu@chemie.uni-marburg.de.

■ ACKNOWLEDGMENT

Financial support by DFG (Priority Program Lanthanoid-Specific Functionality SPP-1166), by Chemetall GmbH, Frankfurt, by Deutscher Akademischer Austauschdienst (DAAD Ostpartnerschaftsprogramm), and by Studienstiftung des Deutschen Volkes is gratefully acknowledged. K.A.R. thanks Prof. Em. Manfred Meisel (Institut für Chemie der Humboldt-Universität zu Berlin) for his munificent support during the stay at his research group and Dr. Brukhard Ziemer for his contribution to the X-ray analysis of **3**.

■ REFERENCES

(1) (a) Edelmann, F. T. *Top. Curr. Chem.* **1996**, *179*, 247–276. (b) Yasuda, H.; Ihara, E. *Bull. Chem. Soc. Jpn.* **1997**, *70*, 1745–1767. (c) Hou, Z.; Wakatsuki, Y. *Coord. Chem. Rev.* **2002**, *231*, 1–22. (d) Molander, G. A.; Romero, J. A. C. *Chem. Rev.* **2002**, *102*, 2161–2185.

(2) (a) Schaverien, C. J. *Adv. Organomet. Chem.* **1994**, *36*, 283–362. (b) Schumann, H.; Meese-Marktscheffel, J. A.; Esser, L. *Chem. Rev.* **1995**, *95*, 865–986. (c) Edelmann, F. T. In *Comprehensive Organometallic Chemistry II*; Abel, E. W.; Stone, F. G. A.; Wilkinson, G., Eds.; Pergamon: Oxford, 1995; Vol. 4, pp 11−212.

(3) (a) Arndt, S.; Okuda, J. *Chem. Rev.* **2002**, *102*, 1953–1976. (b) Hou, Z. *Bull. Chem. Soc. Jpn.* **2003**, *76*, 2253–2266. (c) Gibson, V. C.; Spitzmesser, S. K. *Chem. Rev.* **2003**, *103*, 283–315.

(4) (a) Braunschweig, H.; Breitling, F. M. *Coord. Chem. Rev.* **2006**, *250*, 2691–2720. (b) Cano, J.; Kunz, K. *J. Organomet. Chem.* **2007**, *692*, 4411–4423.

(5) (a) Shapiro, P. J.; Bunel, E. E.; Schaefer, W. P.; Bercaw, J. E. *Organometallics* **1990**, *9*, 867–869. (b) Shapiro, P. J.; Cotter, W. D.; Schaefer, W. P.; Labinger, J. A.; Bercaw, J. E. *J. Am. Chem. Soc.* **1994**, *116*, 4623–4640. (c) Piers, W. E.; Shapiro, P. J.; Bunel, E. E.; Bercaw, J. E. *Synlett* **1990**, *2*, 74–84.

(6) Okuda, J. *Chem. Ber.* **1990**, *123*, 1649–1651.

(7) (a) Stevens, J. C.; Timmers, F. J.; Wilson, D. R.; Schmidt, G. F.; Nickias, P. N.; Rosen, R. K.; Knight, G. W.; Lai, S.-Y. (Dow Chemical Co.) *Eur. Pat. Appl.* EP 0 416 815 A2, 1991. (b) Canich, J. A. M. (Exxon Chemical Co.) *Eur. Pat. Appl.* EP 0 420 436 A1, 1991. (c) McKnight, A. L.; Waymouth, R. M. *Chem. Rev.* **1998**, *98*, 2587–2598.

(8) Petrov, A. R.; Rufanov, K. A.; Ziemer, B.; Neubauer, P.; Kotov, V. V.; Sundermeyer, J. *Dalton Trans.* **2008**, 909–915.

(9) (a) Sundermeyer, J.; Rufanov, K. A.; Petrov, A.; Elfferding, M.; Winkenstette, M. WO/2009/068000, 2009. (b) Sundermeyer, J.; Rufanov, K. A.; Petrov, A.; Elfferding, M.; Winkenstette, M. DE 10 2007 057 854 A1, 2009.

(10) Rufanov, K. A.; Petrov, A. R.; Kotov, V. V.; Laquai, F.; Sundermeyer, J. *Eur. J. Inorg. Chem.* **2005**, 3805–3807.

(11) Freund, C.; Barros, N.; Gronitzka, H.; Martin-Vaca, B.; Maron, L.; Bourissou, D. *Organometallics* **2006**, *25*, 4927–4930.

(12) Oulié, P.; Freund, C.; Saffon, N.; Martin-Vaca, B.; Maron, L.; Bourissou, D. *Organometallics* **2007**, *25*, 6793–6804.

(13) Truflandier, L.; Marsden, C. J.; Freund, C.; Martin-Vaca, B.; Bourissou, D. *Eur. J. Inorg. Chem.* **2004**, 1939–1947.

(14) Petrov, A. R.; Rufanov, K. A.; Hangaly, N. K.; Elfferding, M.; Harms, K.; Sundermeyer, J. *Mendeleev Commun.* **2010**, *20*, 197–199.

(15) For reviews on catalytic hydroamination see: (a) Müller, T. E.; Beller, M. *Chem. Rev.* **1998**, *98*, 675–704. (b) Nobis, M.; Driessen-Hölscher, B. *Angew. Chem.* **2001**, *113* (21), 4105–4108. *Angew. Chem., Int. Ed.* **2001**, *40*, 3983–3985. (c) Pohlki, F.; Doye, S. *Chem. Soc. Rev.* **2003**, *32*, 104–114. (d) Roesky, P. W.; Müller, T. E. *Angew. Chem.* **2003**, *115*, 2812–2814. *Angew. Chem., Int. Ed.* **2003**, *42*, 2708–2710. (e) Hong, S.; Marks, T. J. *Acc. Chem. Res.* **2004**, *37*, 673–686. (f) Hultzsch, K. C. *Adv. Synth. Catal.* **2005**, *347*, 367–391. (g) Hultzsch, K. C. *Org. Biomol. Chem.* **2005**, *3*, 1819–1824. (h) Aillaud, I.; Collin, J.; Hannedouche, J.; Schulz, E. *Dalton Trans.* **2007**, 5105–5118. (i) Severin, R.; Doye, S. *Chem. Soc. Rev.* **2007**, *36*, 1407–1420. (j) Müller, T. E.; Hultzsch, K. C.; Yus, M.; Foubelo, F.; Tada, M. *Chem. Rev.* **2008**, *108*, 3795–3892.

(16) (a) Gagné, M. R.; Marks, T. J. *J. Am. Chem. Soc.* **1989**, *111*, 4108–4109. (b) Gagné, M. R.; Nolan, S. P.; Marks, T. J. *Organometallics* **1990**, *9*, 1716–1718. (c) Gagné, M. R.; Stern, C. L.; Marks, T. J. *J. Am. Chem. Soc.* **1992**, *114*, 275–294.

(17) Representative examples include: (a) Trambitas, A. G.; Panda, T. K.; Jenter, J.; Roesky, P. W.; Daniliuc, C.; Hrib, C. G.; Jones, P. G.; Tamm, M. *Inorg. Chem.* **2010**, *49*, 2435–2446. (b) Stanlake, L. J. E.; Schafer, L. L. *Organometallics* **2009**, *28*, 3990–3998. (c) Lu, E.; Gan, W.; Chen, Y. *Organometallics* **2009**, *28*, 2318–2324. (d) Pawlikowski, A. V.; Ellern, A.; Sadow, A. D. *Inorg. Chem.* **2009**, *48*, 8020–8029. (e) Rastätter, M.; Zulys, A.; Roesky, P. W. *Chem.—Eur. J.* **2007**, *13*, 3606–3616. (f) Gribkov, D. V.; Hultzsch, K. C.; Hampel, F. *J. Am. Chem. Soc.* **2006**, *128*, 3748–3759. (g) Kim, J. Y.; Livinghouse, T. *Org. Lett.* **2005**, *7* (20), 4391–4393. (h) Ryu, J.-S.; Marks, T. J.; McDonald, F. E. *J. Org. Chem.* **2004**, *69*, 1038–1052. (i) Hong, S.; Kawaoka, A. M.; Marks, T. J. *J. Am. Chem. Soc.* **2003**, *125*, 15878–15892. (j) Arredondo, V. M.; Tian, S.; McDonald, F. E.; Marks, T. J. *J. Am. Chem. Soc.* **1999**, *121*, 3633–3639. (k) Li, Y.; Marks, T. J. *J. Am. Chem. Soc.* **1998**, *120*, 1757–1771. (l) Bürgstein, M. R.; Berberich, H.; Roesky, P. W. *Organometallics* **1998**, *17*, 1452–1454. (m) Giardello, M. A.; Conticello, V. P.; Brard, L.; Gagné, M. R.; Marks, T. J. *J. Am. Chem. Soc.* **1994**, *116*, 10241–10254.

(18) Ryu, J.-S.; Li, G. Y.; Marks, T. J. *J. Am. Chem. Soc.* **2003**, *125*, 12584–12605.

(19) (a) Tian, S.; Arredondo, V. M.; Stern, C. L.; Marks, T. J. *Organometallics* **1999**, *18*, 2568–2570. (b) Seyam, A. M.; Stubbert, B. D.; Jensen, T. R., III; J. J., O. D.; Stern, C. L.; Marks, T. J. *Inorg. Chim. Acta* **2004**, *357*, 4029–4035.

(20) Panda, T. K.; Hrib, C. G.; Jones, P. G.; Jenter, J.; Roesky, P. W.; Tamm, M. *Eur. J. Inorg. Chem.* **2008**, 4270–4279.

(21) (a) Edelmann, F. T. *Angew. Chem.* **1995**, *107*, 2647–2669. (b) Edelmann, F. T.; Freckmann, D. M. M.; Schumann, H. *Chem. Rev.* **2002**, *102*, 1851–1896. (c) Zimmermann, M. Z.; Anwander, R. *Chem. Rev.* **2010**, *110*, 6194–6259.

(22) For other spectra see Supporting Information.

(23) Schumann, H.; Glanz, M.; Hemling, H. *J. Organomet. Chem.* **1993**, *445*, C1–C3.

(24) Schumann, H.; Glanz, M.; Hemloing, H.; Hahn, F. E. *Z. Anorg. Allg. Chem.* **1995**, *621*, 341–345.

(25) Hultzsch, K. C.; Voth, P.; Spaniol, T. P.; Okuda, J. *Organometallics* **2000**, *19*, 228–243.

(26) Zhang, W.-X.; Nishiura, M.; Mashiko, T.; Hou, Z. *Chem.—Eur. J.* **2008**, *14*, 2167–2179.

(27) Ghotra, J. S.; Hursthouse, M. B.; Welch, A. J. *J. Chem. Soc., Chem. Commun.* **1973**, 669–670.

(28) Westerhausen, M.; Hartmann, M.; Pfitzner, A.; Schwarz, W. *Z. Anorg. Allg. Chem.* **1995**, *621*, 837–850.

(29) Brady, E. D.; Clark, D. L.; Gordon, J. C.; Hay, P. J.; Keogh, D. W.; Poli, R.; Scott, B. L.; Watkin, J. G. *Inorg. Chem.* **2003**, *42*, 6682–6690.

(30) (a) Tredget, C. S.; Lawrence, S. C.; Ward, B. D.; Howe, R. G.; Cowley, A. R.; Mountford, P. *Organometallics* **2005**, *24*, 3136–3148.
(b) Bambirra, S.; Meetsma, A.; Hessen, B. *Acta Crystallogr., Sect. E* **2006**, *62*, m314–m317.

(31) Emslie, D. J. H.; Piers, W. E.; Parvez, M.; McDonald, R. *Organometallics* **2002**, *21*, 4226–4240.

(32) (a) Evans, W. J.; Brady, J. C.; Ziller, J. W. *J. Am. Chem. Soc.* **2001**, *123*, 7711–7712. (b) Arndt, S.; Zeimentz, P. M.; Spaniol, T. P.; Okuda, J.; Honda, M.; Tatsumi, K. *Dalton Trans.* **2003**, 3622–3627.

(33) Schumann, H.; Freckmann, D. M. M.; Decher, S. *Z. Anorg. Allg. Chem.* **2002**, *628*, 2422–2426.

(34) (a) Beesley, R. M.; Ingold, C. K.; Thorpe, J. F. *J. Chem. Soc., Trans.* **1915**, *107*, 1080–1106. (b) Ingold, C. K. *J. Chem. Soc., Trans.* **1921**, *119*, 305–329. (c) Jung, M. E.; Gervay, J. *J. Am. Chem. Soc.* **1991**, *113*, 224–232. (d) For a review on the Thorpe−Ingold effect see: Sammes, P. G.; Weller, D. J. *Synthesis* **1995**, 1205–1222.

(35) Ge, S.; Meetsma, A.; Hessen, B. *Organometallics* **2008**, *27*, 5339–5346.

(36) Bambirra, S.; Tsurugi, H.; Leusen, D. v.; Hessen, B. *Dalton Trans.* **2006**, 1157–1161.

(37) Gribkov, D. V.; Hultzsch, K. C.; Hampel, F. *Chem.—Eur. J.* **2003**, *9*, 4796–4810.

(38) Gribkov, D. V.; Hampel, F.; Hultzsch, K. C. *Eur. J. Inorg. Chem.* **2004**, 4091–4101.

(39) Stubbert, B. D.; Marks, T. J. *J. Am. Chem. Soc.* **2007**, *129*, 6149–6167.

(40) Dunne, J. F.; Fulton, D. B.; Ellern, A.; Sadow, A. D. *J. Am. Chem. Soc.* **2010**, *132*, 17680–17683.

(41) Arrowsmith, M.; Crimmin, M. R.; Barrett, A. G. M.; Hill, M. S.; Kociok-Köhn, G.; Procopiou, P. A. *Organometallics* **2011**, *30*, 1493–1506.

(42) Manna, K.; Xu, S.; Sadow, A. D. *Angew. Chem., Int. Ed.* **2011**, *50*, 1865–1868.

(43) Allan, L. E. N.; Clarkson, G. J.; Fox, D. J.; Gott, A. L.; Scott, P. *J. Am. Chem. Soc.* **2010**, *132*, 15308–15320.

(44) Tobisch, S. *Chem.—Eur. J.* **2010**, *16*, 13814–13824, and references therein.

(45) Petrov, A. R. Ph.D. Thesis, Marburg/Lahn, Germany, 2008.

(46) (a) Dell'Amico, D. B.; Calderazzo, F.; Porta, C. D.; Merigo, A.; Biagini, P.; Lugli, G.; Wagner, T. *Inorg. Chim. Acta* **1995**, *240*, 1–3. (b) Baisch, U.; Dell'Amico, D. B.; Calderazzo, F.; Conti, R.; Labella, L.; Marchetti, F.; Quadrelli, E. A. *Inorg. Chim. Acta* **2004**, *357*, 1538–1548.

(47) Vaughn, G. D.; Krein, K. A.; Gladysz, J. A. *Organometallics* **1986**, *5*, 936–942.

(48) (a) Bender, C. F.; Widenhoefer, R. A. *J. Am. Chem. Soc.* **2005**, *127*, 1070–1071. (b) Hong, S.; Tian, S.; Metz, M. V.; Marks, T. J. *J. Am. Chem. Soc.* **2003**, *125*, 14768–14783.

(49) *IPDS Software*; Stoe & Cie GMBH: Darmstadt, Germany, 1996.

(50) Blessing, R. H. *Acta Crystallogr.* **1995**, *A51*, 33–38.

(51) Cascarano, G.; Favia, L.; Giacovazzo, C. *SIR 92. J. Appl. Crystallogr.* **1992**, *25*, 310–317.

(52) Altomare, A.; Burla, M. C.; Camalli, M.; Cascarano, G. L.; Giacovazzo, C.; Guagliardi, A.; Moliterni, A. G. G.; Polidori, G.; Spagna, R. *J. Appl. Crystallogr.* **1999**, *32*, 115–119.
(53) Sheldrick, G. M. *SHELXL-97*; University of Göttingen: Germany, 1993.
(54) Spek, A. L. *Acta Crystallogr.* **1990**, *A46*, C34.
(55) Spek, A. L. *Platon: A Multi-Purpose Crystallographic Tool*; Utrecht University: Utrecht, The Netherlands, 2001.
(56) Brandenburg, K. *Diamond*, Release 3.0; Crystal Impact GbR: Bonn, 2004.